# **General Disclaimer**

# One or more of the Following Statements may affect this Document

- This document has been reproduced from the best copy furnished by the organizational source. It is being released in the interest of making available as much information as possible.
- This document may contain data, which exceeds the sheet parameters. It was furnished in this condition by the organizational source and is the best copy available.
- This document may contain tone-on-tone or color graphs, charts and/or pictures, which have been reproduced in black and white.
- This document is paginated as submitted by the original source.
- Portions of this document are not fully legible due to the historical nature of some of the material. However, it is the best reproduction available from the original submission.

Produced by the NASA Center for Aerospace Information (CASI)

Unclas 26047

3746

(Maryland Univ.) CSCL 04A

20

### LUDAR TEMPERATURE PROFILING: PERFORMANCE SIMULATIONS OF MASON'S METHOD

### Geary K. Schwemmer and Thomas D. Wilkerson

When this work was done, both authors were with the University of Maryland, Institute for Physical Science and Technology, College Park, Maryland 20742; G. K. Schwemmer is now with NASA/Goddard Space Flight Center, Earth Observation Systems Division, Greenbelt, Maryland 20771.

19-25619 Several methods of using lasers to measure atmospheric temperature profiles have been described. 1-4 Mason's suggestion 1 is analyzed here to assess its capabilities for various lidar configurations. Temperatures are inferred from a measure of the Boltzmann distribution of rotational states in one of the vibrational bands of 0,. Differential absorption is measured using three tunable, narrowband pulsed lasers. The outputs of two are tuned to wavelengths at the centers of absorption lines at either end of a particular branch in the band. The third wave a length is in a region of no absorption; its liner return measures only the atmo-spheric backscation, and therefore allows one to calculate the absorption coef-ficients at the other two wavelengths as a function of altitude. From the ratio MASONS HETHOD FINAL REPERATURE MASONS HETHOD FINAL REPORT (MATVIAN 10 P HC A02/MF A01 ficients at the other two wavelengths as a function of altitude. From the ratio of the two line absorption coefficients plus a priori knowledge of the line parameters, one can calculate the temperature-altitude profile.

We made computer simulations of various lidar configurations, using different line pairs in the "atmospheric bands" of 02. These bands (~ 630, 690, 760 nm) are likely andidates because the line strengths are sufficient for optimum absorptic. in the troposphere and suratosphere. Also, tunable lasers and photomultipliers for the near IR have improved rapidly in recent years. Results described here are based on the 0, line pair giving the best performance in each situation.

We refer the reases to Schotland<sup>5</sup> for a discussion of differential absorption lidar, and to Mason<sup>1</sup> and Heaton<sup>4</sup> for the expressions relating the ratio of the absorption cross-sections to the standard line parameters:

$$\sigma_1/\sigma_2 = A_1 \exp(-A_2/T)$$

(1)

where  $A_1 = (B_1/B_2)[(2J_1+1)/(2J_2+1)](v_1Y_2/v_2Y_1)$ , and

$$A_2 = (B_0hc/k)[J_1(J_1+1) - J_2(J_2+1)].$$

The  $B_i$  are the Einstein absorption coefficients,  $J_i$  the rotational quantum numbers, and  $v_i$  the line center frequencies; the half widths  $\gamma_i$  are assumed, to first order, to all have the same temperature dependence.<sup>6</sup>  $B_o$  is the rotational constant, <u>h</u> Planck's constant, <u>c</u> the speed of light, and <u>k</u> Boltzmann's constant. The ratio of cross-sections is obtained from the lidar return signals as

$$\frac{\sigma_1(\overline{R})}{\sigma_2(\overline{R})} = \frac{\ln[P_o(R)P_1(R+\Delta R)/P_o(R+\Delta R)P_1(R)]}{\ln[P_o(R)P_2(R+\Delta R)/P_o(R+\Delta R)P_2(R)]}, \quad (2)$$

where the P<sub>o</sub> are the off-line returns and P<sub>1</sub> and P<sub>2</sub> are the on-line returns evaluated at distances R and R+ $\Delta$ R. The range  $\overline{R}$ , at which the average crosssections  $\sigma_i$  are determined, is simply R+ $\frac{\Delta R}{2}$  under the usual assumptions<sup>5</sup> for differential absorption lidar. Note that Eq. (2) does not depend on the number density of the absorbing species; this is an important feature of this method. The number density may be obtained from one of the on-line signals once the temperature profile is known.

To estimate the sensitivity of the technique and estimate the errors and noise in a temperature profile measurement, we solve Eq. (1) for temperature,

$$T = A_2[\ln A_1 - \ln(\sigma_1/\sigma_2)],$$
(3)

and differentiate Eq. (3) about each variable that could contribute significant errors.

Sources of noise considered were photon statistics, background light, and a 1% signal-processing error. Photon noise was usually the major error source in the temperature determination. Only nighttime measurements are considered here because the daytime background in a practical bandwidth of 1 nm is too high for an acceptable signal-to-noise ratio. All of the parameters in the factor  $A_1$  in Eq. (1) are constants; therefore, any uncertainties in these parameters contribute systematically rather than randomly. This uncertainty would be less if the constants were known better, or if one were to use a simultaneous calibration of each lidar signal pulse, similar to that recently employed in a water vapor lidar.<sup>7</sup> Alternatively, a systematic correction could be made to the temperature profile by measuring the temperature in situ somewhere along the line-of-sight. We assumed that the variance in  $A_1$  was  $10^{-3}$ , an optimistic value based on what we considered would be the best obtainable values in a careful measurement of the parameters in  $A_1$ . Present data would give a variance of about  $10^{-2}$ .

While this analysis is for a Lorentz profile(and, strictly speaking, the  $O_2$  lines have a Voigt profile) it provides sufficient accuracy for assessing the errors and practical applications of the method, especially in the troposphere where the lineshape is nearly Lorentzian. The technique is fairly sensitive to temperature. Defining  $U \equiv \sigma_1/\sigma_2$  and differentiating Eq. (1), we see that the fractional change in the ratio of the cross-sections varies with small changes in temperature as

$$\Delta U/U = (A_2/T) (\Delta T/T).$$

Using the J = 1 and J = 19 lines in the P Branch, B Band, and T = 288K, then  $\Delta U/U = .0094 \Delta T$ , about a 1% change per degree. However, performing a similar calculation on Eq. (2), we find that the measurement is very sensitive to noise in the on-line signals. A 1% noise level on each signal gives  $\sim 10\%$  error in the cross-section ratio as calculated from lidar returns.

The parameters used here describe realistic lidar systems, leaning towards the optimistic to allow for technological improvements that are currently underway. The transmitting laser(s) is capable of emitting 300mJ/pulse, simultaneously in each of three wavelengths, two of them narrowband to  $\approx .01$  cm<sup>-1</sup>. The receiver consists of a 1 M<sup>2</sup> collecting telescope and a GaAs photomultiplier. Overall efficiency of the optics is 50%, and the range resolution of the measurements 0.5 - 2.0 is the atmospheric model is a clear mid-latitude summer model.<sup>8</sup> O<sub>2</sub> data were taken from Babcock and Herzberg,<sup>9</sup> Burch and Gryvnak,<sup>10</sup> and Miller, Boese, and Giver.<sup>11-13</sup>

The first lidar configuration considered was ground-based. Errors in the temperature profile measurement are given in Figure 1 as a histogram to show each vertical range element along the profile. Shot noise (dashed line) is the major contributor to the total random error (solid line). At short range, the 1% signal-processing noise (not shown separately) limits the accuracy. This could be improved with quieter, more accurate electronics and finer digitization. Systematic errors from the uncertainty in  $A_1$  (dotted line) may introduce a fairly constant offset of 2-3K. The optimum line pair for lower troposphere profiling from the ground up is (J = 1, J = 19) in the P Branch of the B Band ( $\sim$  690 nm). Measurement accuracy of  $\pm$  lK up to 6 km altitude with 0.5 km resolution is possible when 300 laser pulses are averaged. This is equivalent to about a 30 sec measurement for a large laser system, or 300 sec for a system more typical of the present day.

Another useful lidar platform would be an aircraft or balloon for profiling the troposphere and lower stratosphere (Figure 2). Using the same wave lengths as before, one can profile the troposphere with reasonable accuracy and vertical resolution from an aircraft at 10 km altitude, and an aircraft at 20 km can profile the lower stratosphere. Alternatively, the entire 20 km could be mapped from 20 km by utilizing weaker absorption lines in the  $0_2$ - $\gamma$  Band. The laser signals are not attenuated as rapidly; hence greater penetration depth is possible, with a concomitant loss in vertical resolution and/or temperature accuracy. The receiver collecting area is decreased 10x for the 20 km platform, to simulate what a smaller aircraft such as a U-2 would be able to accommodate. For Space Shuttle experiments, we observe an "error well", typical of satellite lidar simulations, as seen in Figure 3. Errors are large at high altitudes owing to lack of sufficient scattering and absorption to obtain strong signals and detectable absorption. As the number of scatterers and the absorption increase, the errors become smaller at lower altitudes, until the attenuation of the on-line signals becomes so great that the errors increase rapidly again. The location of this "error well" is a strong function of the absorption line strength. The choice of stronger lines goes with measuring at higher altitudes, and weaker lines with lower altitudes. Figure 3 shows what can be done using both less and more laser energy than in Figures 1-2, for the B Band measurements. For this case, improvements in accuracy by increasing laser energy come with great difficulty. Also depicted are the errors in a tropospheric profile using the  $\gamma$  Band and the increased laser energy, and a simulation for the A Band, which gives rather poor results in this case.

1.

This study shows that temperature profiles using Mason's method applied to the red 0<sub>2</sub> bands would be rather coarse when measured from a Space Shuttle lidar, given present expectations for orbital lidar systems. On the other hand, quite adequate temperature profiling in the troposphere and lower stratosphere can be carried out using reasonable lidar systems from ground-based and aircraft/balloon platforms. Recently a new 0<sub>2</sub>-based lidar method has been proposed for temperature<sup>14</sup> and pressure<sup>15</sup> profiling which holds promise for improved Shuttle measurements.

The research summarized here was supported in part by NASA grant NSG-5174 from the Goddard Space Flight Center.

#### References

- 1. J. B. Mason, Applied Optics, 14, 76 (1975).
- W. L. Smith and C.M.R. Platt, "A Laser Method of Observing Surface Pressure and Pressure-Altitude and Temperature Profiles of the Troposphere from Satellites," NOAA Tech. Memo NESS 89 (July 1977).
- 3. A. Cohen, J. A. Cooney, and K. N. Geller, Applied Optics 15, 2896 (1976).
- 4. H. I. Heaton, Astrophysical J., 212, 936 (1977).
- 5. R. M. Scnotland, J. Applied Meto., 13, 71 (1974).
- 6. H. I. Heaton, JOSRT, 16, 801 (1976).
- E. V. Browell, et al., "Development and Evaluation of a Near-IR H<sub>2</sub>O Vapor Dial System," <u>Proc. 8th International Laser Fadar Conference</u>, Drexel Univ., Philadelphia, PA, (June 1977); also, E. V. Browell, T. D. Wilkerson, and T. J. McIlrati, Submitted to Applied Optics, (1979).
- R. A. McClatchey, R. W. Fenn, J.E.A. Selby, F. E. Volz and J. S. Garing, "Optical Properties of the Atmosphere," (Third Edition), AFCRL-72-0497 (1972).
- 9. H. D. Babcock and L. Herzberg, Astrophysical J., 108, 167 (1948).
- 10. D. E. Burch and D. A. Gryvnak, Applied Optics, 8, 1493 (1969).
- 11. J. H. Miller, R. W. Boese, and L. P. Giver, JOSRT, 9, 1507 (1969).
- 12. L. P. Giver, R. W. Boese, and J. H. Miller, JOSRT, 14, 793 (1974).
- 13. J. H. Miller, L. P. Giver, and R. W. Boese, JOSRT, 16, 595 (1976).
- 14. C. L. Korb and C. Y. Weng, "A Two Wavelength Licar Technique for the Measurement of Atmospheric Temperature Profiles," <u>Proc. 9th International</u> Laser Radar Conference, Munich, Germany (1979).
- 15. C. L. Korb and C. Y. Weng, "A Lidar Technique for the Measurement of Atmospheric Pressure Profiles," <u>Proceedings of the American Geophysical</u> Union Spring Meeting, Washington, DC (1979)

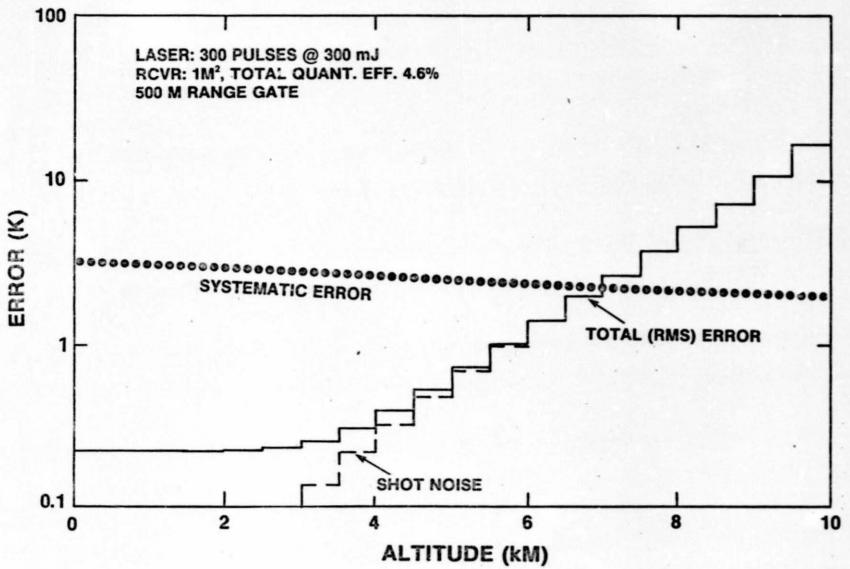
#### Figure Captions (Schwemmer & Wilkerson)

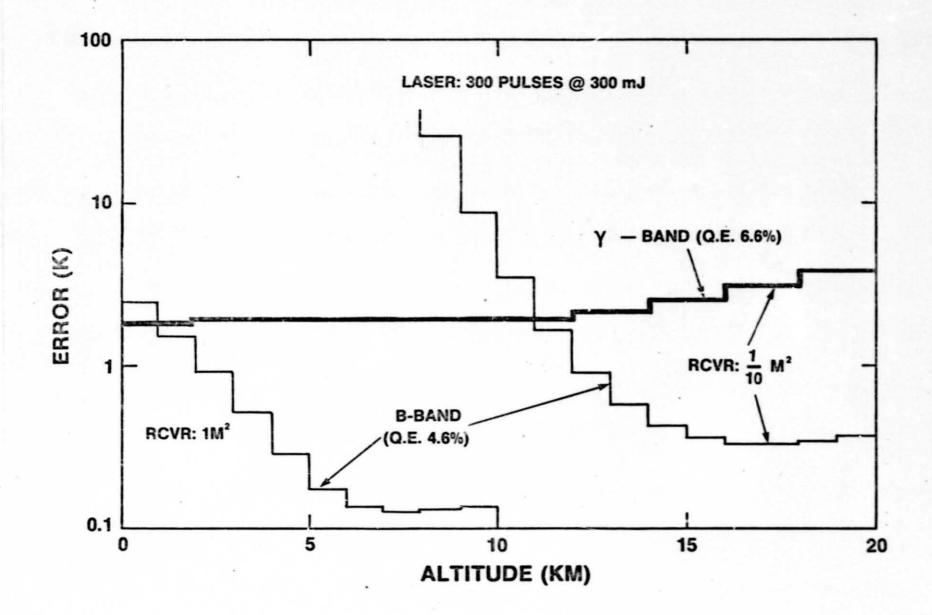
1.

Figure 1. Errors in the lidar temperature profile measured from the ground, using lines J=1 and 19 in the P-branch of the 02 B-band.

Figure 2. Errors in the  $0_2$  temperature profile measured with nadir-viewing lidar in aircraft. B-band profiling from 10 and 20 km (light lines) employs 1 km vertical range resolution and the J=(1,19) line pair in the P-branch.  $\gamma$ -band errors (J=1 and 17) are also shown from the aircraft at 20 km (dark line).

Figure 3. Errors in lidar temperature profiles measured from Space Shuttle. The altitude of optimum accuracy increases with O<sub>2</sub> band strength. Line pairs in the P-branch of each band are J=(1,21)A; (1,19)B; (1,17)Y. A ten-fold decrease in B-band accuracy is shown for a hundred-fold decrease in total laser energy.





X .

